Scientific Visualization, 2023, volume 15, number 3, pages 50 - 57, DOI: 10.26583/sv.15.3.06

Application of Shadow Visualization to Study the Drag of Toroidal Bubbles

E. A. Chashnikov[1], V. V. Nikulin[2]

Lavrentyev Institute of Hydrodynamics SB RAS

[1] ORCID: 0000-0002-1775-1703, chashnikov.e.a@gmail.com
[2] ORCID: 0000-0001-8996-6490, nikulin@hydro.nsc.ru

Abstract

In this work, the ascent of a toroidal bubble created by the injection of a pulsed air jet into water vertically upwards is studied by the shadow method. When using the shadow method, the bubble border on the image is darkened, and the contrast in comparison with the background is increased, which makes it possible to use software processing algorithms to determine the parameters of the ring on each frame. There are experimental results indicating that, in addition to the buoyancy force, the drag force also acts on the toroidal bubble. In this paper, the experimental data on the change in the torus radius as a function of time are compared with a theoretical model constructed with and without taking into account the drag force. It is shown that taking into account the drag force leads to a much better agreement between theory and experiment. The drag force is concluded to act on toroidal bubbles, but its influence decreases with time, i.e., as the bubble rises. The drag coefficient used in the calculations is determined empirically and assumed to be constant.

Keywords: shadow method, toroidal bubble, vortex ring, drag force.

1. Introduction

A toroidal bubble is a type of buoyant vortex rings moving in a liquid, where gas is used as a buoyant substance [1-3]. A distinctive feature of buoyant vortex rings compared to homogeneous ones is the presence of a buoyant force acting on them, which has a significant effect on their dynamics. A large number of works have been devoted to homogeneous vortex rings, where various optical methods are actively used. Thus, the use of optical velocimetry made it possible to study in detail the structure of vortex rings, especially inside the core [4–6]. By PIV method the presence of a vortex ring has been established during direct fuel injection in internal combustion engines [7]. The general state of the human heart was shown in [8] to depend on whether the vortex ring is formed as a result of left ventricle diastole of the heart. Much less attention has been paid to inhomogeneous vortex rings [9–11], including toroidal bubbles. The regularities obtained for toroidal bubbles can be attributed to inhomogeneous vortex rings, although they have distinctive features. One of them is the gas mass conservation, which, under the action of centrifugal forces, is concentrated near the torus circular axis. The peculiar ring structure of toroidal bubbles, together with the rotation of the liquid around the torus, could possibly be useful for intensifying the gas-liquid mass transfer [12], which is encountered in many industrial applications, such as the removal of harmful gases and the capture of CO_2. However, the calculation of the bubble parameters as a function of time according to the available theoretical models [2, 11] does not fully agree with the experiment.

As noted in [13], the dependence of the bubble radius on time, if the bubble is created by injecting an air jet into water, is greater than that obtained experimentally. This may indicate the presence of a drag force acting on the toroidal bubble. It is known that the drag force acting on a bubble in the form of a spherical segment leads to stabilization of its velocity [14, 15]. In the case of homogeneous vortex rings, the drag force does not significantly affect the mo-

tion [16]. The question of the influence of drag on the dynamics of a toroidal bubble remains open.

It should be noted that in [13] a model was proposed taking into account the drag force. However, no comparison with experiment was made, and the calculation of the drag coefficient was performed for only one bubble volume. Thus, the main goal of this study is to test the theoretical model taking into account the drag force, as well as to determine the values of the empirical drag coefficient included into the model for toroidal bubbles with different initial parameters.

2. Theoretical model

The model applied in this paper considers a toroidal bubble rising vertically upward in a gravitational field. The following assumptions are introduced: the bubble has the shape of a torus with parameters R and a, R is the radius of the torus, a is the radius of the cross section of the torus, and $a << R$; the flow around the bubble is irrotational with constant circulation Γ; the volume of the torus is constant and equal to W. According to the assumptions made, the expressions obtained in [2, 17] for the vortex momentum P and the rise velocity V are used:

$$P = \pi\rho\Gamma R^2, \tag{1.1}$$

$$V = \frac{\Gamma}{4\pi R}\left[ln\left(\frac{8R}{a}\right) - \frac{1}{2}\right], \tag{1.2}$$

where ρ is the density of the surrounding liquid.

The differential equation, which can be used to obtain the time dependence of the radius of a toroidal bubble, is derived from the dynamic equation of motion, where, similarly to [13], along with the buoyancy force, the drag force is taken into account in the form:

$$\frac{dP}{dt} = -C_d 2\pi\rho a R V^2 + \rho g W \tag{1.3}$$

where C_d is the drag coefficient.

Without drag force, that is, with $C_d = 0$, from equation (1.3) it is easy to obtain the dependence of the bubble radius on time:

$$R = \left(R_0^2 + \frac{F}{\pi\Gamma}t\right)^{\frac{1}{2}}, \tag{1.4}$$

which is also applicable for inhomogeneous vortex rings with a small density difference between the ring and the environment [11]. In this study, formula (1.4) is used to compare models with and without taking into account the drag force with the experiment.

The length, time, and circulation parameters used below are dimensionless on r_0, $(r_0/g)^{1/2}$, $(gr_0^3)^{1/2}$ respectively, where r_0 is equal to the radius of the ideal sphere containing the same volume of air as a toroidal bubble.

In dimensionless variables, the Cauchy problem with respect to equation (1.3), taking into account (1.1), (1.2) and the constant volume of the bubble $W = 2\pi a^2 R$, takes the form:

$$\frac{dR}{dt} = -C_1\frac{\left[ln\,ln\left(C_2 R\sqrt{R}\right) - \frac{1}{2}\right]^2}{R^2\sqrt{R}} + \frac{C_3}{R}, R(0) = R_0 \tag{1.5}$$

where $C_1 = \frac{\sqrt{6}\Gamma C_d}{(48\pi^2\sqrt{\pi})}$, $C_2 = 4\sqrt{6\pi}$, $C_3 = \frac{2}{(3\Gamma)}$.

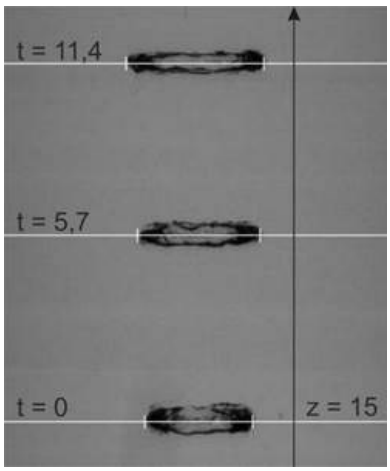

Figure 1. Toroidal bubble ascent, t and z are dimensionless ($\Gamma = 6{,}7; W = 47\ cm^3$).

3. Experimental setup

The experiments were carried out in a water-filled Plexiglas tank 0.5 m long, 0.5 m wide and 1.5 m high. The method for generating toroidal bubbles is as follows. First, compressed air, passing through the pressure regulator, was supplied to the solenoid valve. The open time of the solenoid valve was determined by a programmable logic controller. Moving on, the compressed air flow passed through a mechanical valve, where, pushing the cup against the spring tension, it was injected into the tank. The diameter of the mechanical valve nozzle was 0.4 cm. After injection, the bubble acquired a toroidal shape during the ascent. In the upper part of the tank, the toroidal bubble was captured by a funnel-shaped device for determining the volume of air W. This method for determining the volume allows us to avoid errors associated with perturbations of the bubble surface during formation and movement compared to measurements from images. The volume measurement accuracy is 0.75 ml, which made it possible to measure the volume with an accuracy of 10% for the smallest volume to 1.1% for the largest. The volume of released air was regulated by the pressure of compressed air P and the duration of the open state of the solenoid valve. The pressure took values of 3, 4, 5 and 6 bar, the duration of the open state of the electromagnetic valve varied from 14 to 50 ms. The distance from the nozzle to the lower edge of the funnel-shaped device was 1 m. In the experiments, the volume varied from 7.3 to 70 cm^3.

4. Measuring of ring parameters from images

The shadow registration of the toroidal bubble against the background of a light matte screen was carried out by a high-speed video camera in the direction perpendicular to the motion trajectory with a frequency of 60 fps, an exposure of 750 μs, and a resolution of 1504 × 1128 pixels. When using the shadow method, the bubble border on the image is darkened, and the contrast in comparison with the background is increased, which allows using software processing algorithms to determine the ring parameters on each frame. The resulting videos were processed frame by frame in the Matlab environment using a method similar to that developed earlier and presented in [18]. The main goal of the algorithm from [18] is to find a bubble among all objects in the image and determine the coordinates of the points belonging to it with high accuracy. Figure 1 shows the ring images combination as it moves, where the white lines mark the doubled maximum transverse size of the torus $\boldsymbol{R'}$ found using the algorithm from [18] and its position along the $\boldsymbol{z}$ axis. The $\boldsymbol{z}$-coordinate of the bubble, corresponding to its traveled path from the nozzle, was measured as the arithmetic mean of the coordinates of the points lying on the bubble boundary. To determine the bubble radius $\boldsymbol{R}$, first half of the maximum transverse size of the torus $\boldsymbol{R'}$ was measured in the image.

Then $\boldsymbol{R}$ and $\boldsymbol{a}$ are calculated in terms of $\boldsymbol{R'}$ and $\boldsymbol{W}$ by solving a system of two equations: $\boldsymbol{2\pi^2 R a^2 = W}$, $\boldsymbol{R + a = R'}$. First, we define the boundaries of the range in which physically

correct solutions lie. So, from geometrical considerations, the value of the main radius of the torus $\boldsymbol{R}$ must be greater than the cross-sectional radius $\boldsymbol{a}$, but less than the maximum cross-sectional dimension $\boldsymbol{R'}$, i.e. $\boldsymbol{a = \frac{R'}{2} < R < R'}$. Further, in order to find the only correct solution, we turn to the analysis of the function $\boldsymbol{f(R) = 2\pi^2 R(R - R')^2 - V}$. The maximum point is located at $\boldsymbol{R = \frac{R'}{3}}$ and $\boldsymbol{f\left(\frac{R'}{3}\right) > 0}$, and the minimum point is at $\boldsymbol{R = R'}$ and $\boldsymbol{f(R') < 0}$. Then according to the Bolzano-Cauchy theorem, there is a unique solution on the interval $\boldsymbol{\left(\frac{R'}{3}, R'\right)}$. Thus, the solution of the cubic equation for $\boldsymbol{R \in \left(\frac{R'}{2}, R'\right)}$ is the required one. The measurement error for $\boldsymbol{R'}$ did not exceed 6%. The experimental rate of ascent $\boldsymbol{V}$ is obtained as the ratio of the measured coordinates after a time interval of 1/12 to this interval. This interval is much shorter than the observation time and is sufficient to achieve a measurement accuracy of at least 7% and eliminate sharp fluctuations in the measured velocity. Having determined the experimental rate of rise and the dimensions of the toroidal bubble, the circulation was calculated from expression (1.2):

$$\Gamma = 4\pi RV\left[ln\left(4\sqrt{6\pi}R\sqrt{R}\right) - \frac{1}{2}\right]^{-1} \quad (1.6)$$

Taking into account that the circulation does not change with time, its calculation was carried out at a reference point.

The differential equation (1.5) is solvable for any value of the initial radius R_0. Therefore, the reference point can be chosen at an arbitrary place where the bubble has a toroidal shape. In the experiments performed, the reference point was set at a distance of $15r_0$ from the nozzle. At this distance, in all launches, the bubbles had the torus shape.

Having obtained the dependence of the radius on time and the circulation for one bubble, an estimate of its drag coefficient can be found from the solution of equation (1.5) by comparing the solution with the experimental dependence. Comparison of solutions with different coefficients C_d, which ranged from 0 to 1 with a step of 0.001, was carried out using the least squares method. The best result, that is, C_d such that the discrepancy between solution (1.5) and the experiment was the smallest, was assumed to be the drag coefficient of the given bubble. Note that the proposed method does not provide information on the time dependence of the drag coefficient.

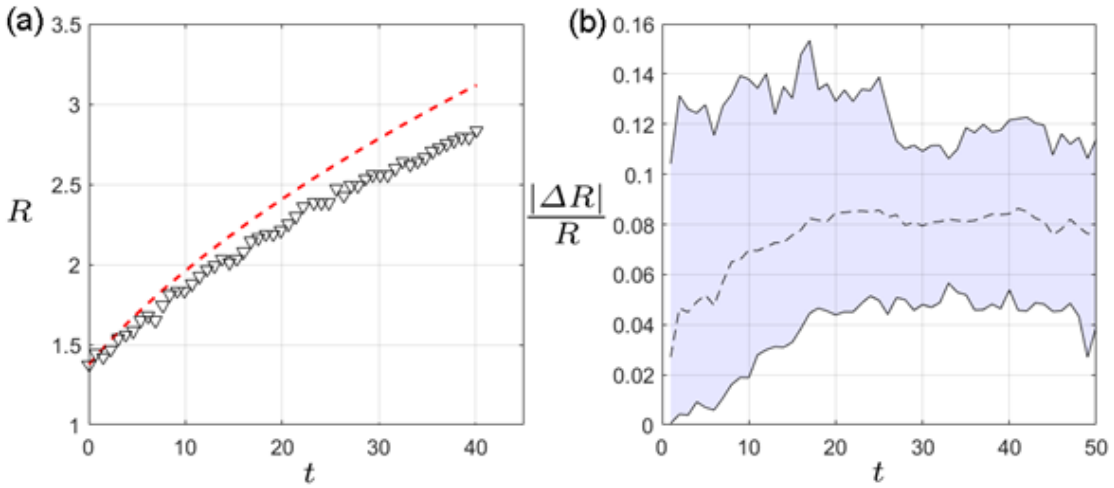

Figure 2. (a) Dependence of radius on time ($\Gamma = 6{,}7; W = 47\ cm^3$): dashed line - calculation by formula (1.4), ∇ - experimental dependence. (b) Averaged over all experiments $|R_{from\ (1.4)} - R_{exp}|/R$, where the dashed line is the average value at time equal to t, the confidence interval of 95% is highlighted in color.

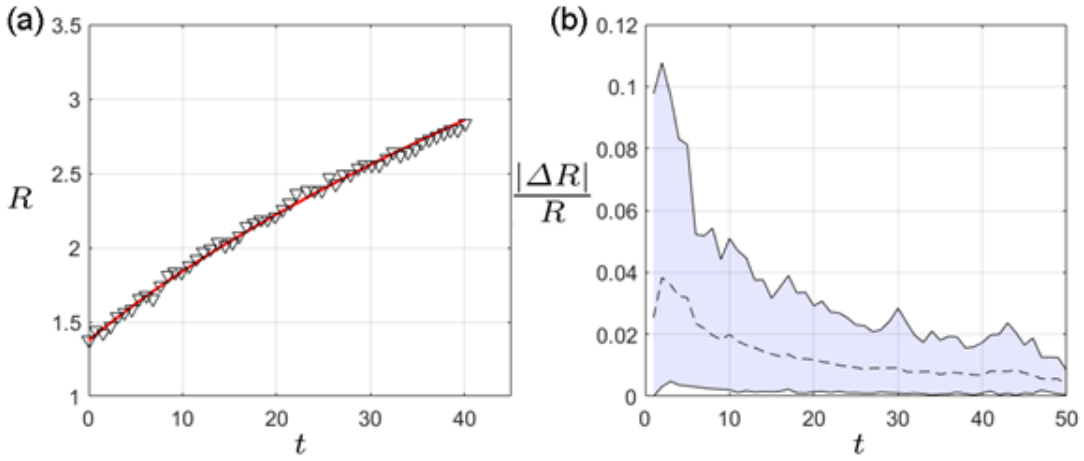

Figure 3. (a) Dependence of radius on time ($\Gamma = 6{,}7; W = 47\ cm^3$): solid line - calculation by formula (1.5) with $C_d = 0{,}248$, ∇ - experimental dependence. (b) Averaged over all experiments $|R_{from\,(1.5)} - R_{exp}|/R$ with C_d, determined by the least squares method, where the dashed line is the average value at time equal to t, the confidence interval of 95% is highlighted in color.

5. Results and discussion

Figures 2(a) and 3(a) show the characteristic experimental points of the core radius against time (∇), at 2(a) data calculated by formula (1.4) (dashed line), at 3(a) data calculated by formula (1.5) with C_d, found by the least square's method (solid line) at $\Gamma = 6{,}7$ and volume $W = 47\ cm^3$. It can be seen that the calculation by formula (1.4) lies above the experimental points, which was observed in all experiments performed. An estimate of the systematic deviation of the calculation according to formulas (1.4) and (1.5) from the experimental points for all bubbles is plotted in figure 2(b) and 3(b). The y-axis shows the ratio of the modules of the difference between theory and experiment with respect to the experiment at the corresponding time t. The density of points distribution at time t is presented through a 95% confidence interval, highlighted in color, where the dashed line means the average value of the relative deviation of theory from experiment. The limits of the confidence interval and the average value at time t were calculated from data from more than 100 bubbles. The comparatively large deviation at t from 0 to 25 relative to the later time is due to the error in determining the radii and the bubble boundaries fluctuation. With time t from 25 onwards, the average and maximum deviation in figure 2(b) is 8-9% and 12-13%, and in figure 3(b) is 0.5-1% and 2-3%, respectively. Thus, including the drag with a constant C_d in the model allows to increase the accuracy of the theoretical calculation several times. It should be noted that the drag coefficient is only assumed to be constant, but in general, it may depend on time. However, taking into account this dependence will not significantly change the calculations accuracy. Since the term responsible for the drag in (1.5) decreases with increasing radius much faster than the buoyancy force. Figure 4 shows the calculated drag coefficients for the corresponding volumes of toroidal bubbles (a) and Froude numbers (b). There is no clear correlation between coefficients and volume, but the drag coefficients seem to correlate with Froude numbers. We define the Froude number in dimensional terms as:

$$Fr = \frac{V^2}{gr_0}, \tag{1.7}$$

in this case, in dimensionless quantities, the Froude number coincides with the squared value of the translational velocity. The toroidal bubble velocity changes as it moves therefore, to compare different experiments, the Froude numbers are calculated at the same distance from the nozzle. The Froude number in figure 4(b) was calculated by (1.7) at the reference point.

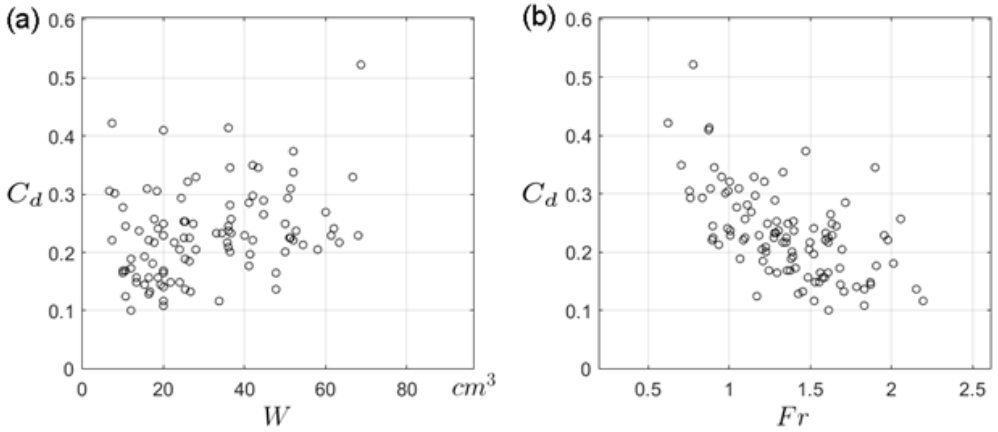

Figure 4. Drag coefficient at corresponding bubble volumes (a) and Froude numbers (b).

6. Conclusion

The ascent of toroidal bubbles is studied for various values of the initial parameters: volume, radius, and circulation. Toroidal bubbles were created by injecting a jet of air vertically into water. The reference point was set at a distance of 15 radii of the sphere, the volume of which is equal to the toroidal bubble volume. It is shown that in this case the dependence of the torus radius on time without taking into account the drag force lies above the experimental points. On a dimensionless time fragment from 0 to 25, the average value of the relative deviation grows to 8-9% and remains constant further. The statistics were collected from measurements of the parameters of more than 100 toroidal bubbles.

A theoretical model was tested, where it is assumed that, in addition to the buoyancy force, a drag force acts on the toroidal bubble. Taking into account the drag force with greater accuracy allows the theoretical calculation to be consistent with the experimental data. The average relative deviation at times 0 to 25 does not exceed 4% and is 0.5-1% further. Thus, we can conclude that, in addition to the buoyancy force, a drag force acts on the toroidal bubble, and it should be taken into account in tasks requiring high accuracy.

The drag coefficient used in the calculations was determined by searching for the best agreement between the calculation and experiment using the least squares method. No clear correlation between drag coefficient and bubble volume is shown. However, it can be seen that an increase in the Froude numbers leads to a decrease in the drag coefficients.

References

1. **Walters J. K., Davidson J. F**. The initial motion of a gas bubble formed in an inviscid liquid // Journal of Fluid Mechanics, Vol. 17, 1963, pp. 321-336.

2. **Pedley T.** The toroidal bubble // Journal of Fluid Mechanics. 1968. V. 32. №. 1. P. 97-112. doi:10.1017/S0022112068000601

3. **Vasel-Be-Hagh A. R., Carriveau R., Ting D. S.-K**. A balloon bursting underwater // Journal of Fluid Mechanics, Vol. 769, 2015, pp. 522-540.

4. **Didden N.** On the formation of vortex rings: Rolling-up and production of circulation // Journal of Applied Mathematics and Physics (ZAMP*)*. 1979. V. 30, P. 101–116. https://doi.org/10.1007/BF01597484

5. **Glezer A., Coles D.** An experimental study of a turbulent vortex ring // Journal of Fluid Mechanics. 1990. V. 211. P. 243-283.

6. **Weigand A., Gharib M.** On the evolution of laminar vortex rings // *Experiments in Fluids*. 1997. V. 22. P. 447–457. https://doi.org/10.1007/s003480050071

7. **Sazhin S.S., Kaplanski F., Feng G., Heikal M.R., Bowen P.J.** A fuel spray induced vortex ring // Fuel. 2001. V. 80. № 13., P. 1871-1883.

8. **Gharib M., Rambod E., Kheradvar A., Sahn D., Dabiri J.** Optimal vortex formation as an index of cardiac health // Proceedings of the National Academy of Sciences of

the United States of America. 2006. V. 103. № 16. P. 6305-8. DOI: 10.1073/pnas.0600520103

9. **Bond D., Johari H.** Impact of buoyancy on vortex ring development in the near field // Experiments in Fluids. 2010. V. 48. P. 737–745. DOI 10.1007/s00348-009-0761-z

10. **Nikulin V., Chashnikov E.** Mass Transfer Between the Vortex Ring and the Surrounding Fluid, when the Density of the Fluid in the Vortex is Less than Outside it // Journal of Siberian Federal University. Mathematics & Physics. 2021. V. 14. № 1. P. 42-46. DOI: 10.17516/1997-1397-2021-14-1-42-46.

11. **Turner J. S.** Buoyant vortex rings // Proceedings of the Royal Society of London. Series A. Mathematical and Physical Sciences. 1957. V. 239. P. 61 – 75

12. **Ma Y., Guocong Y., Huai Z. L.** Note on the Mechanism of Interfacial Mass Transfer of Absorption Processes // International Journal of Heat and Mass Transfer. 2005. V. 48. № 16. P. 3454-3460. https://doi.org/10.1016/j.ijheatmasstransfer.2005.03.008

13. **Vasel-Be-Hagh A.R., Carriveau R., Ting D. S.K., Turner J.S.** Drag of buoyant vortex rings // Physical Review E. 2015. V. 92. № 4. P. 043024

14. **Бэтчелор Дж.** Введение в гидродинамику жидкости. М.: Мир, 1973. 758 с.

15. **Davis R.M., Taylor G.I.** The mechanism of large bubbles rising through liquids in tubes // Proceedings of the Royal Society of London. Series A. *1950*. V. 200. P. 375-390.

16. **Sullivan I., Niemela J., Hershberger R., Bolster D., Donnelly R.** Dynamics of thin vortex rings // *Journal of Fluid Mechanics*. 2008. V. *609*. P. 319-347. doi:10.1017/S0022112008002292

17. **Saffman P.G.** The velocity of viscous vortex rings // Studies in Applied Mathematics. 1970. V. 49. № 4. P. 371-380.

18. **Chashnikov E.A., Nikulin V.V.** Determination of the Parameters of a Vortex Ring with an Air Core in a Liquid by Computer Processing of Video Images // Scientific Visualization. 2021. V 13.3. P. 66-74. DOI: 10.26583/sv.13.3.07